

# Lattice Dynamics in a strongly dimerized low-dimensional Model with Orbital Ordering

A. Friedrich<sup>1,\*</sup> and W. Brenig<sup>2</sup>

<sup>1</sup>*RWTH Aachen, Institut für Theoretische Physik C, Physikzentrum, 52056 Aachen*

<sup>2</sup>*Technische Universität Braunschweig, Institut für Theoretische Physik, Mendelssohnstr. 3, 38106 Braunschweig*

(Dated: 11th November 2018)

We study the interplay of spin, orbital and lattice degrees of freedom in a one-dimensional Kugel-Khomskii model coupled to phonons. In the vicinity of the dimer point we analyze the excitation spectrum, mapping the spin and orbital degrees of freedom to bond operators. In particular we study the renormalization of the phonon propagator due to coupling to the orbital and magnetic excitations. Considering both, ferro- and antiferro-orbital ordering we will show that the appearance of orbiton shake-up processes in the phonon spectrum is sensitive to the type of Jahn-Teller distortion. The relevance of our results for optical spectroscopy on low dimensional transition metal compounds will be discussed.

## I. INTRODUCTION

Orbital ordering in three dimensions (3D) is a well established phenomenon in a variety of transition-metal compounds<sup>1</sup>. Very recently, quasi one-dimensional (1D) systems with potentially similar behavior, such as  $\text{Na}_2\text{Ti}_2\text{Sb}_2\text{O}_7$ <sup>2</sup> and  $\text{NaTiSi}_2\text{O}_6$ <sup>3</sup> have attracted considerable interest. In these systems the coupling of orbital degrees of freedom to those of the spin and probably also to the lattice have been suggested to lead to a rich variety of possible phases and non-trivial elementary excitations<sup>4</sup>. In principle the orbitally ordered state will allow for elementary excitations of orbital nature, i.e. *orbitons*. However, while their existence has been predicted more than two decades ago<sup>5</sup> it has been only very recently that an indirect observation of orbitons in 3D has been claimed in shake-up side-bands of Raman-active phonon spectra in  $\text{LaMnO}_3$ <sup>6</sup>. This observation underlines the relevance of a simultaneous description of orbital and lattice degrees of freedom. Unfortunately however, for quasi 1D materials this is still an open issue. It is the aim of this work to investigate the phonon spectra of a 1D model of mixed orbital and spin degrees of freedom by investigating its harmonic lattice dynamics in the vicinity of two specifically chosen Jahn-Teller (JT) distortions. The outline of the paper is as follows. In section I we discuss the 1D spin-orbital Hamiltonian and its excitations using a bond-operator method close to the so-called dimer line. Sections II and III will focus on the phonon-spectra which form in the presence of a frozen-in, either ferro- or antiferro-orbital JT distortions. Conclusions will be presented in the final section IV. Technical details are deferred to appendices A through D.

## II. BOND-OPERATOR DESCRIPTION OF THE 1D KUGEL-KHOMSKII MODEL

In this section, and prior to discussing their effect on the lattice dynamics we develop a description of the orbital and spin excitations. In the limit of strong Coulomb

repulsion, orbital degeneracy in the Hubbard model can be described in terms of a pseudo-spin model, as was shown several decades ago by Kugel and Khomskii<sup>5</sup>. In 1D and for a two-fold orbital degeneracy at 1/4-filling this leads to the Hamiltonian of a magnetic spin-1/2 chain coupled to an orbital pseudo-spin-1/2 chain by bi-quadratic interactions

$$H = J_1 \sum_n S_n^\alpha S_{n+1}^\alpha + J_2 \sum_n (T_n^\alpha T_{n+1}^\alpha + A T_n^z T_{n+1}^z) + K \sum_n S_n^\alpha S_{n+1}^\alpha (T_n^\gamma T_{n+1}^\gamma + B T_n^z T_{n+1}^z) \quad (1)$$

where, apart from the spin-1/2 operator  $S_n$ , a pseudo spin-1/2 variable  $T_n$  with  $T_n^z = \pm 1/2$  corresponding to the orbital degrees of freedom is attached to each site 'n'. Summation over the spin indices  $\alpha = x, y, z$  and  $\gamma = x, y, z$  is implied. In the remainder of this paper energies will be given in units of  $K$ .

The quantum phase diagram of (1) has been the subject of intense research<sup>4,7,8,9,10,11</sup>. For  $J_1, J_2 > 1/4$  its spectrum is believed to be massive<sup>7</sup>. At  $J_1 = J_2 = 1/4$  and  $A = B = 0$  the model has  $\text{SU}(4)$  symmetry and is integrable<sup>4</sup>. Along the 'dimer line'  $J_1 = (3+A)/4$ ,  $J_2 = 3/4$  with  $-2 < A < \infty$  it displays a two-fold degenerate, fully dimerized ground state. At the 'dimer point'  $J_1 = J_2 = 3/4$  this ground state can be expressed as a direct matrix-product of alternating spin and orbital singlets with an energy gap of  $\Delta \sim 0.375$ <sup>7,9,11</sup>. Exactly on the dimer line the elementary excitations are massive solitons, i.e. domain walls between the two-fold degenerate ground-states. However, off from the dimer-line the latter readily bind to form generalized gapful triplet-modes<sup>9</sup>.

Prior to including the effects of a JT-distortion we now reformulate (1) in terms of bosonic bond-operators<sup>12,13,14</sup>. This allows for an approximate description of the formation of the spin and orbital singlets in the ground state of the dimer phase

$$S_{2,n}^\alpha = \frac{1}{2} (\pm s_n^\dagger t_{\alpha,n} \pm t_{\alpha,n}^\dagger s_n - i \epsilon_{\alpha\beta\gamma} t_{\beta,n}^\dagger t_{\gamma,n}) \\ T_{2,n}^\alpha = \frac{1}{2} (\pm \sigma_n^\dagger \tau_{\alpha,n} \pm \tau_{\alpha,n}^\dagger \sigma_n - i \epsilon_{\alpha\beta\gamma} \tau_{\beta,n}^\dagger \tau_{\gamma,n}) \quad (2)$$

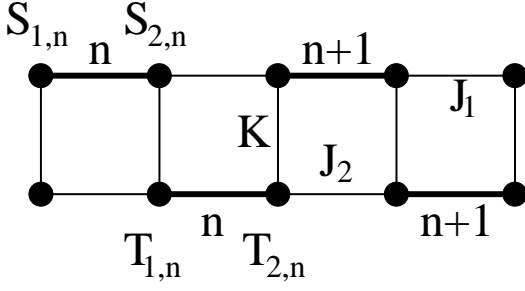


Figure 1: Dimer representation of the spin-orbital chain.  $n$  labels the dimer, the index 1,2 the site on a dimer. On each site on the upper (lower) chain sits one spin  $S_{i,n}$  (pseudo-spin  $T_{i,n}$  i.e. orbital degree of freedom) respectively.

where  $s(\sigma)_n^{(\dagger)}$  and  $t(\tau)_n^{(\dagger)}$  create/destroy spin(orbital) singlets and triplets and the index 1(2) labels the left (right) site of the dimer  $n$  in Fig. 1. Bose operators labeled by roman letters refer to spin space, while greek ones refer to orbital space. The bond-operators have to satisfy

$$s(\sigma)_n^\dagger s(\sigma)_n + t(\tau)_{\alpha,n}^\dagger t(\tau)_{\alpha,n} = 1 \quad (3)$$

which implies the constraint of no double-occupancy of the bonds by singlets or triplets.

Inserting (2) into (1) an interacting Bose gas is obtained. In the limit of strong dimerization one may proceed with the latter by invoking the Holstein-Primakoff (LHP) approximation<sup>12,14</sup>. I.e. the singlets are removed using (3) and assuming  $s^{(\dagger)}$  and  $\sigma^{(\dagger)}$  to be  $C$ -numbers. This is consistent with a condensation of the singlets in the ground state, i.e. the formation of a dimer state. The procedure leads to square roots of type  $s^{(\dagger)}(\sigma^{(\dagger)}) = [1 - t(\tau)_{\alpha,n}^\dagger t(\tau)_{\alpha,n}]^{1/2}$  which, approximately, may be linearized to retain triplet interactions up to quartic order. Since we are interested in the effects of mutual interactions between the orbital and magnetic sector we simplify even further, by keeping those interactions which mix the orbital and magnetic triplets, but discarding quartic terms of purely orbital or magnetic nature. After some algebra we find a quadratic part of the Hamiltonian

$$H_0 = -\frac{N}{4} [3(J_1 + J_2) + J_2 A] + \sum_{n,m,i,j} \Phi_{n,i}^* M_{n,m}^{ij} \Phi_{m,j} \quad (4)$$

with  $\Phi_n = (t_{\alpha,n}^\dagger, t_{\alpha,n}, \tau_{x,y,n}^\dagger, \tau_{x,y,n}, \tau_{z,n}^\dagger, \tau_{z,n})$  and again  $\alpha = x, y, z$ .  $n$  and  $m$  label dimers and  $i$  and  $j$  the components of  $\Phi^*$  and  $\Phi$ . The matrix elements  $M_{n,m}^{ij}$  are given in Appendix A. We note, that on the quadratic level no mixing occurs between the spin and orbital triplets. For

the quartic spin-orbital interactions we get

$$H_{SO} = -\frac{1}{4} \sum_n \left\{ \left[ \tau_{z,n}^\dagger \tau_{z,n} + \left(1 + \frac{B}{2}\right) \tau_{\beta,n}^\dagger \tau_{\beta,n} \right] \times \left( t_{\alpha,n-1}^\dagger t_{\alpha,n} + t_{\alpha,n-1}^\dagger t_{\alpha,n}^\dagger + h.c. \right) \right\} - \frac{1}{4} (1+B) \sum_n \left[ t_{\alpha,n}^\dagger t_{\alpha,n} \times \left( \tau_{z,n-1}^\dagger \tau_{z,n} + \tau_{z,n-1}^\dagger \tau_{z,n}^\dagger + h.c. \right) \right] - \frac{1}{4} \sum_n t_{\alpha,n}^\dagger t_{\alpha,n} \left( \tau_{\beta,n-1}^\dagger \tau_{\beta,n} + \tau_{\beta,n-1}^\dagger \tau_{\beta,n}^\dagger + h.c. \right) \quad (5)$$

with  $\beta = x, y$ . The quadratic part  $H_0$  can be diagonalized by Fourier- and Bogoliubov transformation leading to dispersions

$$H_{LHP} = \sum_{k,\alpha,x} \omega_{x,k} x_{k,\alpha}^\dagger x_{k,\alpha} \quad (6)$$

$$\omega_{x,k} = \chi_{1,x} [\chi_{2,x} + \chi_{3,x} \cos(k)]^{\frac{1}{2}}, \quad (7)$$

where  $x = a, c$  label new quasi-particles of purely spin ( $a$ ) and orbital ( $c$ ) nature with  $t_{\alpha,k}^\dagger = u_k a_{\alpha,k}^\dagger + v_k a_{\alpha,-k}$  and  $\tau_{\alpha,k}^\dagger = g_k c_{\alpha,k}^\dagger + h_k c_{\alpha,-k}$ . Explicit expressions for the dispersions  $\omega_{x,k}$ , the Bogoliubov coefficients, and  $\chi_{i,x}$  are listed in Appendix B. After Fourier-transformation the spin-orbital interaction  $H_{SO}$  reads<sup>15</sup>

$$H_{SO} = \sum_{k,k',q} \left[ a_{\alpha,k'-q}^\dagger a_{\alpha,-k'}^\dagger \times \left( V_{k,k',q}^{1,\gamma} c_{\gamma,k+q}^\dagger c_{\gamma,-k}^\dagger + V_{k,k',q}^{2,\gamma} c_{\gamma,k+q}^\dagger c_{\gamma,k}^\dagger \right) + h.c. \right] + \sum_{k,k',q} \left[ a_{\alpha,k'-q}^\dagger a_{\alpha,k'}^\dagger \times \left( V_{k,k',q}^{3,\gamma} c_{\gamma,k+q}^\dagger c_{\gamma,-k}^\dagger + V_{k,k',q}^{4,\gamma} c_{\gamma,k+q}^\dagger c_{\gamma,k}^\dagger \right) + h.c. \right], \quad (8)$$

where  $\gamma = x, y, z$  and the  $V_{k,k',q}^{i,\gamma}$  are rather lengthy expressions given in Appendix D.

At the points of complete dimerization and in a pure spin system the bond-boson description is characterized by a vanishing of the inter-dimer coupling. This is *not* the case in the spin-orbital chain, i.e., even at the dimer-point  $J_{1,2}=3/4$ , the matrix elements  $V_{k,k',q}^{i,\gamma}$  do not vanish and the sum of (4) and (8) remains a non-trivial interacting problem. In turn, spin-triplets can excite orbital-triplets by virtue of  $H_{SO}$  and vice versa. For an approximate account of the resulting renormalization of the one particle excitations, we include the effects of  $V_{k,k',q}^{i,\gamma}$  perturbatively up to second order in the self energy. The one particle excitations result form the poles of the matrix Green's function

$$\mathbf{G}_\nu = \begin{pmatrix} G_{\nu,11} & G_{\nu,12} \\ G_{\nu,21} & G_{\nu,22} \end{pmatrix} = \mathbf{G}_\nu^0 + \mathbf{G}_\nu^0 \Sigma_\nu \mathbf{G}_\nu, \quad (9)$$

where the second index-pair refers to normal (11 and 22) and anomalous (12 and 21) propagators for particles of

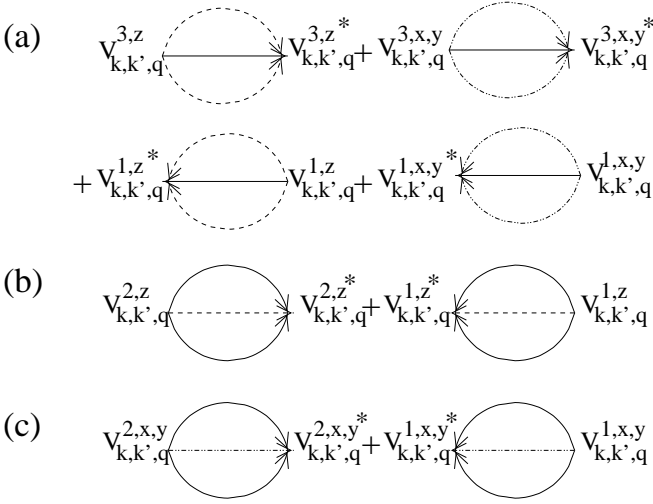


Figure 2: Self energy of the spin and orbital triplet Green's functions. (a)  $\Sigma_{a_{x,y,z}}(k, \omega)$  (b)  $\Sigma_{c_z}(k, \omega)$  (c)  $\Sigma_{c_{x,y}}(k, \omega)$ . Full lines denote  $G_{a_{x,y,z}}^0(k, \omega)$ , dashed lines  $G_{c_z}^0(k, \omega)$  and dotted lines  $G_{c_{x,y}}^0(k, \omega)$ .

type  $\nu$ , where  $\nu = a_{x,y,z}$  or  $\nu = c_{x,y,z}$  labels spin or orbital triplets. Because  $\mathbf{G}_\nu^0$  is calculated from  $H_{LHP}$  it is diagonal, i.e.  $G_{\nu,12}^0 = G_{\nu,21}^0 = 0$ . For the non-diagonal elements of  $\mathbf{G}_\nu$  this does not apply because the matrix-self energy  $\Sigma_\nu$  is not diagonal. Fig. 2 depicts all contributions to  $\Sigma_\nu$  up to second order, where each diagram occurs with both, an incoming and an outgoing propagator on either side, i.e. such that the self energy corrections can be written in terms of a  $2 \times 2$ -matrix notation for each of the 3 orbital and 3 spin triplets. These diagrams show that the spin(orbital) triplet motion is renormalized by emission of two orbital(spin) triplets. Earlier variational calculations, performed in ref. 16 have been based on a *subset* consisting of exactly these intermediate states. We have evaluated the self energy contributions of Fig. 2 numerically. The dressed Green's function spectrum displays undamped triplet quasi-particles as well as a three-particle continuum. Close to the dimer point their respective spectral ranges are well separated. In Fig. 3 we show the dispersion of the quasi-particles only. For comparison this figure contains complementary data from exact diagonalization(ED)<sup>16</sup>. Firstly, within a finite range of momenta around the zone center and apart from a global relative shift of the spectra by  $\sim 0.1$ , reasonable agreement can be observed for the low-energy excitations, i.e. the  $\tau_z$  orbital-triplets. Secondly, with respect to the LHP, inclusion of the self-energy from Fig. 2 improves the agreement with ED. Thirdly, close to the zone boundary the ED spectrum refers to the lower edge of the orbital two-soliton continuum, rather than the orbital triplet, i.e. the two-soliton bound-state<sup>16</sup>. This two-soliton continuum is lacking in the approximate bond-operator approach.

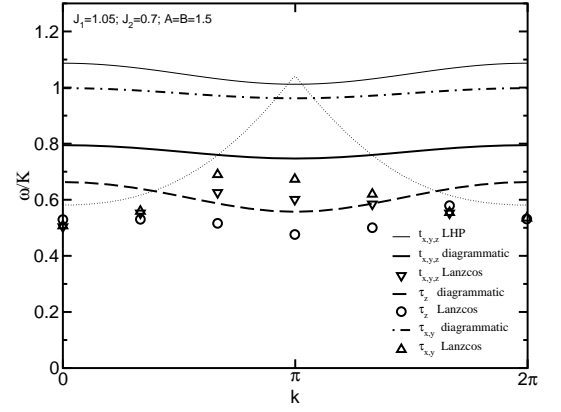


Figure 3: Self energy corrected triplet dispersions of the spin-orbital chain. Full lines: spin triplets with (thick line) and without (thin line) self-energy corrections. Dashed line: orbital  $z$ -triplets. Dot-dashed line: orbital  $x,y$  triplets. The dotted line show the border of the multi-soliton continuum<sup>16</sup>. The symbols denote the spin and orbital triplet energies obtained by exact diagonalization studies (Lanczos) for a system of the length 12 (rungs)<sup>16</sup>. ED momenta have been back-folded into the dimerized Brillouine.

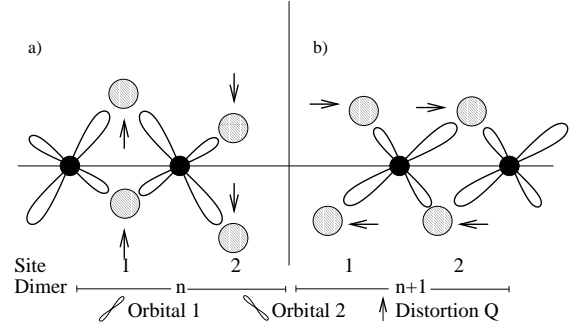


Figure 4: Chosen phonon modes. a) transverse distortion leading to antiferro-orbital ordering and b) longitudinal distortion leading to ferro-orbital ordering. The loops labeled orbital one/two denote the  $3d_{yz}/3d_{zx}$  orbital respectively. The hatched circles symbolize super-exchange orbitals of p-symmetry. Also shown is the static distortion  $Q$ . The different size of the orbitals denote the different Coulomb repulsion by electrons belonging to neighboring atoms: the larger an orbital is drawn, the lower is its energy.

### III. LATTICE DYNAMICS

We are now in a position to consider the phonon-renormalization due to orbital and spin excitations. To this end two steps are required. Firstly, the equilibrium structure of the lattice in the orbitally ordered ground state has to be clarified. Secondly, the lattice dynamics has to be evaluated. The first step is specific to the material. Here we focus on a situation compatible with  $\text{Na}_2\text{Ti}_2\text{Sb}_2\text{O}$  where the  $3d_{yz/zx}$ -orbitals form the 1D chain-structures, shown in Fig. 4<sup>2,17</sup>. Several static Jahn-Teller-type distortions could be envisaged lifting the orbital degeneracy. In the remainder of this paper we

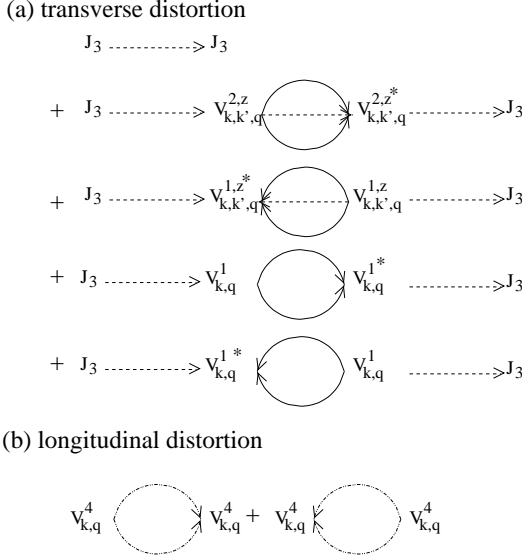


Figure 5: Self energy of the phonon propagator with (a) transverse and (b) longitudinal distortion. As in Fig. 2 full lines denote  $G_{a_{x,y,z}}^0(k, \omega)$ , dashed lines  $G_{c_z}^0(k, \omega)$  and dotted lines  $G_{c_{x,y}}^0(k, \omega)$ . Note, that  $G_{c_z}^0(k, \omega)$  is calculated with the shifted  $\tilde{\tau}_{z,k}^{(\dagger)}$  (see eq. 12) instead of the pure  $\tau^{(\dagger)}$ , that was used in the calculations without any distortion. The explicit expressions for the different  $V_{k,k',q}^{i,z}$ ,  $i = 1, 2$  and  $V_{k,q}^j$ ,  $j = 1, 4$  are given in appendix D.

confine the discussion to the homogeneous *ferro*(or *longitudinal*)- and *antiferro*(or *transverse*)-orbital static and dynamic distortion (c.f. Fig. 4a) and b)). The phonon-orbital contribution to the Hamiltonian for both of Fig. 4a) and b) reads

$$H_{phon} = \sum_n (Q + J_3 (b_n^\dagger + b_n)) (T_{1,n}^z \pm T_{2,n}^z) + \omega_{b,k} b_k^\dagger b_k, \quad (10)$$

Both phonon modes couple to the  $z$ -component of the orbital pseudo-spin operator  $T$ , where '-' and '+' refer to the transverse, i.e. Fig. 4a), and longitudinal, i.e. Fig. 4b), phonon mode.  $Q$  accounts for the static Jahn-Teller distortion,  $b_{n(k)}^{(\dagger)}$  are phonon destruction(creation) operators at site(momentum)  $n(k)$  and  $\omega_{b,k}$  is the bare phonon dispersion.

### A. Transverse distortion

First we consider the transverse mode of Fig. 4a), associated with antiferro-orbital ordering (AF-OO). In this case the electrons on two neighboring sites occupy alternating orbitals. Expressing  $T_1^z$  and  $T_2^z$  in terms of bond-

operators and after Fourier transformation (10) reads:

$$H_{trans}^{phon} = \sum_k Q(\tau_{z,0} + \tau_{z,0}^\dagger) + J_3 \underbrace{(b_k^\dagger \tau_{z,k} + b_{-k} \tau_{z,k} + h.c.)}_{b)} + \omega_{b,k} b_k^\dagger b_k, \quad (11)$$

with a total Hamiltonian of  $H = H_{LHP} + H_{SO} + H_{trans}^{phon}$ . The contribution linear in  $\tau_{z,0}$  resulting from the static distortion, i.e. a) in (11), can be eliminated by realizing that  $H_{LHP}$  is quadratic in  $\tau_{z,k}^{(\dagger)}$  and by invoking a constant shift of the latter operators through:

$$\tau_{z,k}^{(\dagger)} \rightarrow \tilde{\tau}_{z,k}^{(\dagger)} - \frac{Q\delta_{k,0}}{(1 + J_2 - (J_2 - \frac{3}{4} + J_2 A - \frac{3}{4} B) \cos k)}. \quad (12)$$

On the level of the LHP this does not modify the  $\tau_z$ -dispersion. However, inserting (12) into  $H_{SO}$  of (5), new hopping terms for the spin triplets are generated modifying their dispersion. Moreover, additional three-triplet vertices occur, because of which orbital triplets now couple to a two-spin-triplet-continuum. These new terms read

$$H_{SO}^{new} = \sum_{k,q} V_{k,q}^1 (c_{z,k}^\dagger a_{x,y,z,q}^\dagger a_{x,y,z,-k-q}^\dagger + c_{z,-k}^\dagger a_{x,y,z,-q} a_{x,y,z,k+q} + h.c.) + \sum_{k,q} V_{k,q}^2 (c_{z,k}^\dagger a_{x,y,z,q}^\dagger a_{x,y,z,k+q} + h.c.) \quad (13)$$

They lead to additional self-energy contributions for the Green's function of the orbital triplets which have to be included in the phononic self-energy because of the coupling of the orbital triplets to the phonons. Explicit expressions for the resulting spin-triplet dispersion  $\tilde{\omega}_{\gamma,k}$  on the quadratic level, as well as the matrix elements  $V_{k,q}^i$  with  $i = 1, 2$  of this new spin-orbital interaction are given in appendix C and appendix D, respectively. In Fig. 6 we show  $\tilde{\omega}_{\gamma,k}$  for various values of  $Q$  at the dimer point. As is obvious, the static Jahn-Teller distortion leads to a finite triplet dispersion.

To evaluate the phonon propagator  $G_{b_k, b_k^\dagger}(k, \omega)$  we use the Dyson equation (9) with the self energy depicted in Fig. 5. This includes corrections up to second order in the phonon-orbital-spin interactions. The phonon spectrum  $S_b(k, \omega)$  is then defined as

$$S_b(k, \omega) = -\frac{1}{\pi} \text{Im} G_{b_k, b_k^\dagger}(k, \omega). \quad (14)$$

Due to the alternation of the lattice distortion in the AF-OO case, i.e. the '-'-sign in (10), there is only a linear coupling of the phonon to the orbital  $z$ -triplets in (11). Therefore, the dominant renormalization of the phonon-spectrum is a direct mixing between  $z$ -orbitons and phonons. The remaining self-energy corrections

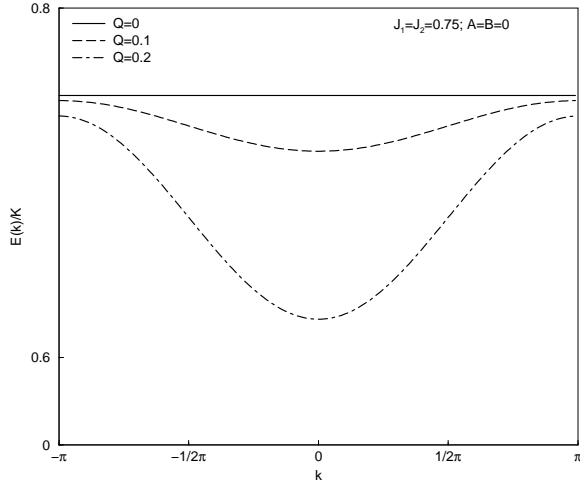


Figure 6: Self-energy-corrected spin triplet dispersion without (full line) and with different (dashed and dot-dashed lines) strength of distortion  $Q$  at the dimer point.

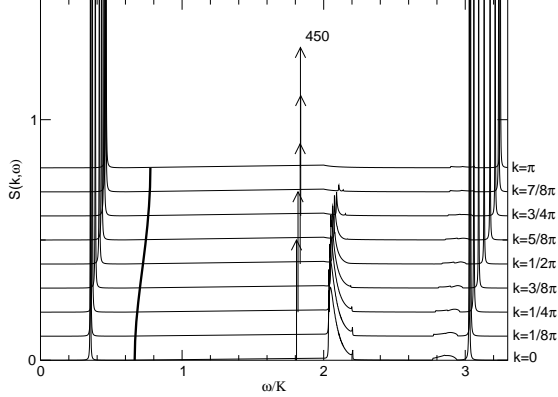


Figure 7: Phonon spectrum  $S_b(k, \omega)$  at  $J_1 = 1.2$ ,  $J_2 = 0.8$ ,  $A = B = 1.5$ ,  $J_3 = 0.35$  and  $\omega_b = 1.8$  calculated with  $\eta = 0.001$ . The left peak is the one-orbital excitation peak, strongly shifted to lower energies by the distortion of the system. Note the peak position without any distortion (thick black line). The position of the phonon-energy peak is shown by up-arrows. Because it is an undamped pole of the phonon Green's function it is a  $\delta$ -peak, the height of which is given for one example in the figure. Its width is set by the numerical broadening  $\eta$ . The two-particle continuum at  $\omega \approx 2.0 - 2.2$  shows the two van-Hove singularities one expects for a continuum of two non-interacting particles. At  $\omega \approx 2.75 - 3.3$  one finds the three-particle continuum.

which are shown in Fig. 5(a) lead to two- and three-particle continua.

Figure 7 depicts the results of a numerical calculation of the phonon-spectrum. In this figure the bare orbion and phonon energies have been chosen to be well separated, with a phonon-energy above the orbion one. First, the spectrum displays two one-particle peaks which are simple poles of the phonon Green's function, i.e. the renormalized phonon and orbion. Their widths are set

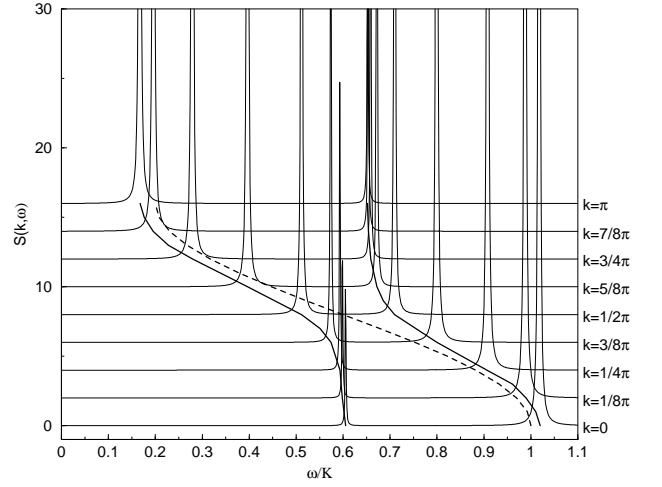


Figure 8: The phonon peak in the phonon propagator spectrum crossing the orbion energy at the dimer point, i.e.  $J_1 = J_2 = 0.75$ ,  $A = B = 0$  with  $\omega_b = (0.6 + 0.4 \cos k)$   $Q = 0.1$  and  $\eta = 0.001$ . The dotted line shows  $\omega_b$  as it is set, while the thick full lines denote the peak position of the two quasi-particles. The quasi-particle excitations at  $k \approx \pi/2$  are mixtures of orbions and phonons as expected for interacting particles.

by an arbitrarily small numerical parameter  $i\eta$ . The bare phonon energy is momentum independent, i.e.  $\omega_b = 1.8$ . This energy remains almost unrenormalized, acquiring a very small dispersion and an upward-shift. The energy of the orbion-peak is clearly lowered with respect to its bare position (thick solid line in Fig. 7). This shift increases with increasing  $Q$ , rendering the AF-OO unstable at sufficiently large values of the static distortion. Apart from the one-particle peaks Fig. 7 displays the anticipated two- and three-particle continua. Their relative weight, as well as the momentum dependence of their shape - which exhibits characteristic van-Hove singularities - is determined by the matrix elements of (8) listed in appendix D.

For dispersive phonons, a crossing of the bare phonon and orbion dispersion may occur, where however phonon-orbion coupling will lead to level repulsion in the renormalized spectra as shown in Fig. 8. In that case the quasi-particles in the vicinity of  $k = \pi/2$  correspond to an approximately equal-amplitude mixture with even and odd parity of orbions and phonons.

## B. Longitudinal distortion

Now we consider the longitudinal mode of Fig. 4 b), which we associate with ferro-orbital ordering (F-OO). After a Fourier and Bogoliubov transformation and inserting the bond-boson expression for  $T_1^z$  and  $T_2^z$  (10)

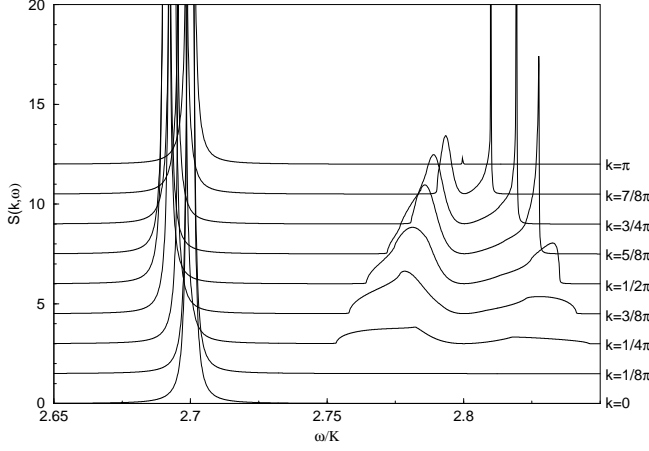


Figure 9: Spectrum of the phonon propagator in the system distorted with the longitudinal distortion. Here the parameters are  $J_1 = 1.2$ ,  $J_2 = 0.8$ ,  $A = B = 1.5$ ,  $J_3 = 0.3$ ,  $\omega_b = 2.7$ ,  $Q = 0.1$  and  $\eta = 0.0001$ . Note that there is no feature except the phonon-peak at  $k = 0$ . This means this kind of distortion will not be seen in spectra of optical experiments.

reads

$$H_{long}^{phon} = -2iQ \sum_k c_{x,k}^\dagger c_{y,k} - c_{y,k}^\dagger c_{x,k} \quad (15)$$

$$+ V_{k,q}^3 (b_q^\dagger + b_{-q}) \left( c_{x,k}^\dagger c_{y,k+q} - c_{y,-k-q}^\dagger c_{x,-k} \right)$$

$$+ V_{k,q}^4 (b_q^\dagger + b_{-q}) \left( c_{x,k}^\dagger c_{y,-k-q}^\dagger - c_{y,k+q} c_{x,-k} \right).$$

Again the exact expressions for  $V_{k,q}^i$  with  $i = 3, 4$  are given in appendix D. This leads to the diagrams shown in Fig. 5b) for the longitudinal distortion. The contribution of (15) which is static with respect to the distortion lifts the degeneracy of the orbital  $x$ - and  $y$ -triplets. This leads to new triplet operators  $c_{1(2),k} = +(-)ic_{x,k} + c_{y,k}$  with an energy-splitting of  $\Delta\omega_c = 4Q$ . Yet, to simplify matters the phonon-propagator is evaluated discarding this effect, using the Bogoliubov transformed  $x$ - and  $y$ -orbital-triplets of (6).

While for the AF-OO a linear coupling of phonons and orbitons results from (10), the '-'-sign in the latter eqn. leads to (15), i.e. the decay of phonons into orbital triplet-pairs in the case of F-OO. In turn the primary effect on the phonon spectrum in the F-OO is the appearance of the a two-orbion continuum. This can be observed in Fig. 9 which depicts the numerical solution of the Dyson equation of Fig. 5 b). The spectrum shows a renormalized simple phonon-pole the width of which is set by a numerical broadening of  $i\eta = i10^{-4}$ . The weak phonon-dispersion observable is an interaction effects, since the bare phonon has been chosen to be purely optical. In addition to the renormalized phonon Fig. 9 exhibits a two-orbion continuum, the spectral weight of which is more than one order of magnitude larger than for the AF-OO case. In the case of the finite splitting  $\Delta\omega_c$

included Fig. 9 would show three superimposed continua, a case which we leave to future analysis. As for the AF-OO the continuum shows characteristic van-Hove type singularities. Most important however, at momentum  $k = 0$  the spectrum resembles a pure phonon excitation only. This is caused by a vanishing of the matrix element  $V_{k,q}^4$  at  $q = 0$  (see App. D) and implies that this kind of distortion will not have any effect on spectra of optical experiments e.g. Raman-scattering.

#### IV. CONCLUSION

In conclusion we have studied the interplay of spin, orbit and lattice dynamics in a model of an anisotropic spin-orbital coupled chain in the vicinity of the dimer-point. The spin-orbital sector of this model has been treated by mapping onto interacting bond-bosons with a singlet condensate and massive triplet modes. We have analyzed the lifting of the orbital degeneracy for two kinds of dynamic Jahn-Teller distortions leading either to antiferro- or ferro-orbital ordering. Studying the phonon dynamics in both cases we have found shake-up sidebands which are critically dependent on the type of distortion. In particular we have found (no) optical activity of the phonon in the transverse (longitudinal) distortion.

**Acknowledgment:** We thank C. Jurecka for stimulating discussions in the beginning of this work. This research was supported in part by the DFG, Schwerpunktprogramm 1073.

#### Appendix A: MATRIX ELEMENTS OF $H_0$

For the matrix elements of the quadratic part of the Hamiltonian (Eq. 4) one finds  $M_{n,n}^{12} = J_1$ ,  $M_{n,n}^{34} = J_2(1 + A/2)$ ,  $M_{n,n}^{56} = J_2$ ,  $M_{n+1,n}^{12} = M_{n+1,n}^{21} = M_{n+1,n}^{11} = M_{n+1,n}^{22} = -1/4(J_1 - 3/4 - 1/4B)$ ,  $M_{n-1,n}^{34} = M_{n-1,n}^{43} = M_{n-1,n}^{33} = M_{n-1,n}^{44} = -1/4(J_2 - 3/4)$  and  $M_{n-1,n}^{56} = M_{n-1,n}^{65} = M_{n-1,n}^{55} = M_{n-1,n}^{66} = -1/4(J_2(1 + A) - 3/4(1 + B))$ . All the other matrix elements are zero.

#### Appendix B: SPIN AND ORBITAL TRIPLET-DISPERSIONS AND BOGOLIUBOV COEFFICIENTS

Here the spin and orbital triplet dispersions after LHP approximation (7) are given.

$$\omega_{a,k} = J_1 \left[ 1 - \left( 1 - \frac{3}{4J_1}(1 + B) \right) \cos k \right]^{\frac{1}{2}}$$

$$\omega_{c_{x,y},k} = J_2 \left[ \left( 1 + \frac{A}{2} \right)^2 - \left( 1 + \frac{A}{2} \right) \left( 1 - \frac{3}{4J_2} \right) \cos k \right]^{\frac{1}{2}}$$

$$\omega_{c_z,k} = J_2 \left[ 1 - \left( 1 - \frac{3}{4J_2}(1 + B) + A \right) \cos k \right]^{\frac{1}{2}} \quad (B1)$$

The Bogoliubov coefficients are defined as

$$\begin{aligned} u_k^2 &= \frac{1}{2} \left[ 1 + \frac{J_1 - \frac{1}{2}(J_1 - \frac{3}{4} - \frac{1}{4}B) \cos k}{\omega_{\gamma,k}} \right] \\ g_k^2 &= \frac{1}{2} \left[ 1 + \frac{J_2 - \frac{1}{2}(J_2(1+A) - \frac{3}{4}(1+B)) \cos k}{\omega_{z,k}} \right] \\ m_k^2 &= \frac{1}{2} \left[ 1 + \frac{J_2(1 + \frac{A}{2}) - \frac{1}{2}(J_2 - \frac{3}{4}) \cos k}{\omega_{l,k}} \right] \end{aligned} \quad (\text{B2})$$

and  $v_k^2 = u_k^2 - 1$ ,  $h_k^2 = g_k^2 - 1$ ,  $n_k^2 = m_k^2 - 1$ .

### Appendix C: SPIN-TRIPLET DISPERSION FOR STATIC TRANSVERSAL DISTORTION

For the spin-triplet dispersion  $\tilde{\omega}_{\gamma,k}$  for the static transversal distortion one finds:

$$\begin{aligned} \tilde{\omega}_{\gamma,k} &= \left[ -\frac{64Q^2(4(1+B)u_kv_k + (u_k + v_k)^2 \cos k)}{(7+3B-4AJ_2)^4} \right. \\ &\quad \left. + \left( \omega_{\gamma,k} - \frac{8Q^2(2(1+B)(u_k^2 + v_k^2) + (u_k + v_k)^2 \cos k)}{(7+3B-4AJ_2)^2} \right)^2 \right]^{\frac{1}{2}}. \end{aligned} \quad (\text{C1})$$

where  $\omega_{\gamma,k}$  is the spin triplet dispersion of the undistorted model and  $u_k$  and  $v_k$  are the Bogoliubov-coefficients (Appendix B) of the transformations in (6)

### Appendix D: MATRIX ELEMENTS OF THE SPIN-ORBITAL INTERACTION $H_{so}$

For completeness the matrix elements of the spin orbital interaction (8) are listed. Here  $T_{x,y} = e^{-ix} + e^{i(x-y)}$ . With  $u_k + v_k = w_k$ ,  $g_k + h_k = i_k$ ,  $m_k + n_k = o_k$ ,  $u_k u_{k'} + v_k v_{k'} = W_{k,k'}$ ,  $g_k g_{k'} + h_k h_{k'} = I_{k,k'}$ ,  $m_k m_{k'} + n_k n_{k'} = O_{k,k'}$  and  $1+B = B_1$ ,  $1+B/2 = B_2$ :

$$\begin{aligned} V_{k,k',q}^{1,z} &= -\frac{1}{8}[(2T_{k',q} + 2B_1 T_{k,-q}^*)g_{k+q}h_k u_{k'-q}v_{k'} \\ &\quad + T_{k',q}(g_{k+q}h_k u_{k'-q}u_{k'} + h_{k+q}g_k v_{k'-q}v_{k'}) \\ &\quad + B_1 T_{k,-q}^*(g_{k+q}g_k u_{k'-q}v_{k'} + \\ &\quad + u_{k'}v_{k'-q}h_{k+q}h_k)] \end{aligned} \quad (\text{D1})$$

$$\begin{aligned} V_{k,k',q}^{1,x,y} &= -\frac{1}{8}[(2B_2 T_{k',q} + 2T_{k,-q}^*)m_{k+q}n_k u_{k'-q}v_{k'} \\ &\quad + B_2 T_{k',q}(m_{k+q}n_k u_{k'-q}u_{k'} + n_{k+q}m_k v_{k'-q}v_{k'}) \\ &\quad + T_{k,-q}^*(m_{k+q}m_k u_{k'-q}v_{k'} + \\ &\quad + u_{k'}v_{k'-q}n_{k+q}n_k)] \end{aligned} \quad (\text{D2})$$

$$\begin{aligned} V_{k,k',q}^{2,z} &= -\frac{1}{8}[T_{k',q}I_{k+q,k}w_{k'-q}w_{k'} \\ &\quad + 2B_1 T_{k,-q}^*u_{k'-q}v_{k'}i_{k+q}i_k] \end{aligned} \quad (\text{D3})$$

$$\begin{aligned} V_{k,k',q}^{2,x,y} &= -\frac{1}{8}[B_2 T_{k',q}O_{k+q,k}w_{k'-q}w_{k'} \\ &\quad + 2T_{k,-q}^*u_{k'-q}v_{k'}o_{k+q}o_k] \end{aligned} \quad (\text{D4})$$

$$\begin{aligned} V_{k,k',q}^{3,z} &= -\frac{1}{8}[2T_{k,-q}g_{k'-q}h_{k'}w_{k+q}w_k \\ &\quad + B_1 T_{k',q}^*W_{k+q,k}i_{k'-q}i_{k'}] \end{aligned} \quad (\text{D5})$$

$$\begin{aligned} V_{k,k',q}^{3,x,y} &= -\frac{1}{8}[B_2 2T_{k,-q}m_{k'-q}n_{k'}w_{k+q}w_k \\ &\quad + T_{k',q}^*W_{k+q,k}o_{k'-q}o_{k'}] \end{aligned} \quad (\text{D6})$$

$$\begin{aligned} V_{k,k',q}^{4,z} &= -\frac{1}{4}[(T_{k',q} + B_1 T_{k,-q}^*)I_{k+q,k}W_{k',k'-q} \\ &\quad + T_{k',q}(u_{k'-q}v_{k'} + v_{k'-q}u_{k'})I_{k+q,k} \\ &\quad + B_1 T_{k,-q}^*W_{k'-q,k'}(g_{k+q}h_k + h_{k+q}g_k)] \end{aligned} \quad (\text{D7})$$

$$\begin{aligned} V_{k,k',q}^{4,x,y} &= -\frac{1}{4}[(T_{k',q}B_2 + T_{k,-q}^*)O_{k+q,k}W_{k',k'-q} \\ &\quad + B_2 T_{k',q}(u_{k'-q}v_{k'} + v_{k'-q}u_{k'})O_{k+q,k} \\ &\quad + T_{k,-q}^*W_{k'-q,k'}(m_{k+q}n_k + n_{k+q}m_k)]. \end{aligned} \quad (\text{D8})$$

The matrix elements of the spin-orbital interaction  $H_{so}$  arising from the shifted orbital triplets are:

$$\begin{aligned} V_{k,q}^1 &= \frac{1}{4}F \sum_{k,q} [\cos q \cdot f_k \cdot (W_{k,k+q}) + \\ &\quad + (\cos q + \cos(k+q) + 2(1+B) \cdot (1 + \cos k)) \times \\ &\quad \times (g_k u_q v_{k+q} + h_k v_q u_{k+q})] \end{aligned} \quad (\text{D9})$$

$$\begin{aligned} V_{k,q}^2 &= \frac{1}{4}F \sum_{k,q} [2 \cos q \cdot (i_k) \cdot (u_k v_{k+q} + v_q u_{k+q}) + \\ &\quad + (\cos q + \cos(k+q) \cdot 2 \cdot (1+B) \cdot (1 + \cos k)) \times \\ &\quad \times (i_k) \cdot (W_{k,k+q})] \end{aligned} \quad (\text{D10})$$

$$V_{k,q}^3 = -2iO_{k,k+q} \quad (\text{D11})$$

$$V_{k,q}^4 = 2i(m_k n_{k+q} - m_{k+q} n_k) \quad (\text{D12})$$

where  $F = Q/((J_2 + 4X)\omega_{b,0} + 4J_2^2)$ ,  $X = -1/4(J_2 - 3/4 + J_2 A - 3/4 B)$  and  $u_k$ ,  $v_k$ ,  $g_k$ ,  $h_k$ ,  $m_k$ ,  $n_k$  are the Bogoliubov-coefficients (Appendix B) of the transformations in (6).

\* Electronic address: afried@physik.rwth-aachen.de

<sup>1</sup> E. Dagotto, *Nanoscale Phase Separation and Colossal Magneto-resistance*, Springer-Verlag Berlin-Heidelberg

(2003).

<sup>2</sup> E. A. Axtell, III *et al.*, J. Solid State Chem. **134**, 423 (1997).

- <sup>3</sup> M. J. Konstantinović and J. v.d. Brink and Z. V. Popović and V. V. Moshchalkov and M. Isobe and Y. Ueda, cond-mat/0210191 (2002).
- <sup>4</sup> P. Azaria and E. Boulat and P. Lecheminant, Phys. Rev. B **61**, 12112 (2000).
- <sup>5</sup> K. I. Kugel and D. I. Khomskii, Sov. Phys. Usp. **25**, 231 (1982).
- <sup>6</sup> E. Saitoh *et al.*, Nature **410** 180 (2001).
- <sup>7</sup> S. K. Pati and R. R. P. Singh, Phys. Rev. Lett. **81**, 5406 (1998).
- <sup>8</sup> B. Frischmuth and F. Mila and M. Troyer, Phys. Rev. Lett. **82**, 835 (1999).
- <sup>9</sup> A. K. Kolezhuk and H. J. Mikeska, Phys. Rev. Lett. **80**, 2079 (1998).
- <sup>10</sup> Y. Yamashita and N. Shibata and K. Ueda, Phys. Rev. B **58**, 9114 (1998).
- <sup>11</sup> C. Itoi and S. Qin and I. Affleck, Phys. Rev. B **61** 6747 (2000).
- <sup>12</sup> O. A. Starykh and M. E. Zhitomirsky and D. I. Khomskii and R. R. P. Singh and K. Ueda, Phys. Rev. Lett. **77**, 2558 (1996).
- <sup>13</sup> S. Sachdev and R. N. Bhatt, Phys. Rev. B **41**, 9323 (1990).
- <sup>14</sup> W. Brenig, Phys. Rev. B **56**, 14441 (1997).
- <sup>15</sup> C. Jurecka, *Excitations in Electron Systems with strongly dimerized Ground States*, PhD-thesis, Cuvillier-Verlag Göttingen (2001), ISBN 3-89873-273-8.
- <sup>16</sup> A. K. Kolezhuk and H.-J. Mikeska and U. Schollwöck, Phys. Rev. B **63**, 064418 (2001).
- <sup>17</sup> M. V. Mostovoy and D. I. Khomskii, Phys. Rev. Lett. **89**, 227203 (2002).